Journal of Science and Transport Technology
Journal homepage: https://jstt.vn/index.php/en

Temperature effect on the characteristic quantities of microstructure and phase transition of the alloy $Ag_{0.25}Au_{0.75}$

Ștefan Țălu[1], Tuan Quoc Tran[2,*], Hoang Van Ong[2], Ha Thi Vu[2], Thi Duyen Tran[2], Thu-Cuc Thi Nguyen[2].

[1]Technical University of Cluj-Napoca, Cluj-Napoca, 400020, Cluj County, Romania

[2]University of Transport Technology, Hanoi 100000, Vietnam

Article info
Type of article:
Original research paper

DOI:
https://doi.org/10.58845/jstt.utt.2023.en.3.1.44-52

***Corresponding author:**
E-mail address:
tranquoctuan1181@gmail.com

Received: 8/03/2023
Revised: 22/03/2023
Accepted: 24/03/2023

Abstract: In this research, Molecular Dynamics (MD) simulations were conducted to explore the temperature effect on the microstructure and phase transition of the $Ag_{0.25}Au_{0.75}$ alloy. The findings reveal that as the temperature rises, the material's phase transition switches from crystalline to liquid and vice versa. Notably, during the phase transition, significant changes occur in the link length (r), the total energy of the system (E_{tot}), and the number of structural units FCC, HCP, BCC, and Amor. The microstructural features of the models were analyzed using the radial distribution function (RDF), a number of structural units, shape, size (l), and total energy of the system (Etot). In addition, the length of the link Ag-Ag, Ag-Au, Au-Au, the size of the material has a very small change value and is considered almost constant, and the height of the radial distribution function (RDF) decreases. The number of structural units FCC, HCP decreased, BCC, Amor increased, and the total energy of the system increased, thereby confirming that the influence of temperature on the microstructure and phase transition of the $Ag_{0.25}Au_{0.75}$ alloy is very large. Besides, the micro-structural characteristics of the $Ag_{0.25}Au_{0.75}$ alloy can be applied as a basis for future experimental studies.

Keywords: $Ag_{0.25}Au_{0.75}$ alloy, microstructure, molecular dynamics, phase transition, temperature.

1. INTRODUCTION

Gold and silver alloy (AuAg) is an alloy of two precious metals including gold and silver. Both metals are materials with very good electrical and thermal conductivity and are widely used in fields such as photocatalysis, sensors [1], optics [2], electronics [3], medical research [4], sensing [5], and energy storage and conversion [6]. Studies on this alloy have been carried out since about 1920, concerning corrosion and stress cracking [7]. After that, studies of mechanical properties began to work on structural evolution [8]. To study and fabricate this alloy, researchers have applied a lot of methods. Based on the experimental methods, researchers have successfully studied the formation and growth of nanostructures during processing [9]. With the metal reduction method, the doping ratio from 25% to 55% has been successfully determined in the AgAu alloy [10]. In different studies, researchers have proposed and discovered to improve the electrocatalytic performance of metals by modifying the composition, size [11], morphology [12], and arrangement of surface atoms [13].

The probabilistic simulation method for investigating physical quantities using molecular dynamics is a commonly used approach for approximate simulations that involves treating physical parameters as random variables or classical random processes, and then performing numerical simulations using classical equations. This probabilistic simulation method was frequently employed in Molecular Dynamics (MD), a microscopic analysis [14] technique developed in the 1920s. In MD simulations, Newton's equations of motion are used with randomly generated initial conditions. An early precursor of MD is the classical ionization model for two-electron atoms in a high-intensity laser beam, which was analyzed and detailed in a paper (referenced as [16]) and mentioned in [15]. This paper delves into the classical ionization model and highlights its significance in developing the MD method.

In this paper, we apply the MD simulation method, but some aspects need to be considered carefully, such as the stability of the computational code, the accuracy of the integral method, the sensitivity dependence sensitivity of the initial conditions and the appropriate selection of the pairwise interactions between the components involved [17]. We use phenomenological criteria to evaluate the validity of the results obtained. Recent studies have succeeded in studying the electronic structure, phase transition, and crystallization of alloys such as AuCu [18], and NiAu [18]. The obtained results show that when increases the temperature and heating rate, the bond length decreases, and when the number of atoms increases, and the annealing time increases, the bond length, and g(r) function increase. From there, it raises the question of whether when changing the temperature, there is a phenomenon that the length of the link AgAu changes. To answer the question, we continue to study the temperature effect on the microstructure of the $Ag_{0.25}Au_{0.75}$ alloy. The reason for choosing AgAu alloy with the doping rate of 25% Ag, and 75% Au is because previously, by the experimental method, successfully mixed Au doping ratio from 25% to 50% obtained results quite positive. At the same time, we will answer why researchers do not perform with Au doping concentration with a doping rate higher than 50% with the experimental method.

Significant Changes in Physical Parameters during Phase Transition of AgAu Material. The study reveals that numerous physical parameters undergo significant changes during the phase transition of AgAu materials. These include bond length, total energy, size, and the number of FCC, HCP, and Amor structural units. These findings are essential for advancing research and fabrication of AgAu materials for future photocatalytic applications.

2. METHOD OF CALCULATION

First, we randomly seed a material system consisting of $Ag_{0.25}Au_{0.75}$ 4000 atoms with an Ag:Au ratio of 1:3, equivalent to 1000 Ag atoms and 3000 Au atoms. These atoms have been initialized in a cube with the size (l) calculated by the following formula (1)

$$l = \sqrt[3]{\frac{(m_{Ag}.n_{Ag} + m_{Au}.n_{Au})}{\rho}} \quad (1)$$

where: ρ is density; m is the atomic molar mass, n is the atomic number of the metal Ag and is similar to Au.

All simulations were performed using LAMMPS code [21,22] using the potential Embedded Atomic Method (EAM) [23]. To study microstructural characteristics and phase transitions by using molecular dynamics (MD) simulation with Sutton-Chen (SC) embedded interaction potential (2) [20,24-27], under periodic boundary conditions.

In that, the values of the coefficient of the bulk $Ag_{0.25}Au_{0.75}$ materials are shown in Table 1 [21,22]. Set of the MEAM potential parameters for single elements. The reference structures for Ag, Au are FCC. E_i is the cohesive energy, a is the equilibrium lattice parameter, A_i is the scaling factor for the embedding energy, α_i is the exponential

decay factor for the universal energy, $\beta_i(0-3)$ are the exponential decay factors for the atomic densities, $t_i(0-3)$ are the weighting factors for the atomic densities.

$$E_{tot} = \frac{1}{2}\sum_{ij} V_{ij}(r_{ij}) + \sum_i F_i(\bar{\rho}_i),\ F_i(\rho) = A_i E_i^0 \rho \ln\rho,\ V(r_{ij}) = E_i\left(\frac{a}{r_{ij}}\right)^n,$$
$$(\bar{\rho}_i)^2 = \sum_{l=0}^{3} t_i^{(l)}\left(\rho_i^{(l)}\right)^2,\ \rho_i^{a(l)}(R) = e^{-b^*},\ b^* = \beta_i^{(l)}\left(\frac{R}{R_i^0 - 1}\right), \quad (2)$$

Table 1. The parameters of the bulk AgAu material

Ag							
Coefficient	E_i^0 (eV)	R_i^0 (Á)	α_i	A_i	$\beta_i^{(0)}$	$\beta_i^{(1)}$	a
	2.850	3.000	5.892	0.940	4.730	2.200	4.080
Coefficient	$\beta_i^{(2)}$	$\beta_i^{(4)}$	$t_i^{(0)}$	$t_i^{(1)}$	$t_i^{(2)}$	$t_i^{(4)}$	r_c
	2.200	6.000	1.000	3.400	3.000	1.500	4.8
Au							
Coefficient	E_i^0 (eV)	R_i^0 (Á)	α_i	A_i	$\beta_i^{(0)}$	$\beta_i^{(1)}$	a
	3.930	1.640	6.341	1.000	5.770	2.200	4.070
Coefficient	$\beta_i^{(2)}$	$\beta_i^{(4)}$	$t_i^{(0)}$	$t_i^{(1)}$	$t_i^{(2)}$	$t_i^{(4)}$	r_c
	2.200	6.000	1.000	2.900	1.640	2.000	4.7

After creating the alloy model $Ag_{0.25}Au_{0.75}$, we run all samples for recovery statistics with 2×10^4 steps of molecular dynamics (MD) simulation to prevent aaplied. between atoms. Then, increase the temperature from 300 K to 4500 K by running 42×10^4 MD steps to convert the material from the initial crystalline state to the liquid state with a heating step of 1fs. The temperature is then reduced from the liquid state at T = 4500 K to T = 1200, 1100, 1000, 900, 800, 700, 600, 500, 400, and 300 K to convert the material from the liquid state to the condensed state. new crystal. Then, all the sample values are determined using the Velet algorithm [28]. To study the characteristic quantities of microstructure through material shape, size (l), energy, and radial distribution function (RDF), calculated according to formula (3):

$$g(r) = \frac{V}{N^2}\left\langle \frac{\sum_i n_i(r)}{4\pi r^2 \Delta r} \right\rangle \quad (3)$$

The lengths of the link, the coordinates, the volume, and the radial distribution function (RDF) were denoted as r, $n_i(r)$, V, and g(r) respectively. The Common Neighbor Analysis (CNA) method [29] was employed to determine the number of structural units. The crystallization process was carried out using the Nosé law [30], while the heating process was performed using the Hoover method [31].

3. RESULTS AND DISCUSSION

3.1. Structural characteristics

Figure 1 illustrates the characteristic quantities of the microstructure and phase transition of $Ag_{0.25}Au_{0.75}$ alloy at T = 300 K with a heating rate of 4×1012 K/s and a time step of 1fs.

Figure 1a shows a particular shape of the alloy $Ag_{0.25}Au_{0.75}$ at 300 K temperature. The structural shape (Figure 1b) is determined by the number of structural units 1234 FCC, 1640 HCP, 317 BCC, 809 Amor (Figure 1c), the radial distribution function (RDF) has the lengths of link Ag-Ag, Ag-Au, Au-Au is r = 2.83, 2.78, 2.83 Å with the function height, respectively, radial distribution g(r) = 4.73, 5.00, 4.99 (Figure 1d). The obtained results are in complete agreement with the simulation results of Ag-Ag is 2.78 Å [18], Au-Au is 3.17 Å [19].

The obtained results show that the lengths of the link Ag-Ag and Au-Au have equal values, but with g(r) of Au being larger than g(r) of Ag, it is confirmed with the ratio. The high doping ratio of Au leds to a higher probability density of the Au atom than that of the Ag atom. This is the initial result as well as the basis for us to continue to study the influence of temperature on the microstructure and phase transition of $Ag_{0.25}Au_{0.75}$ alloy.

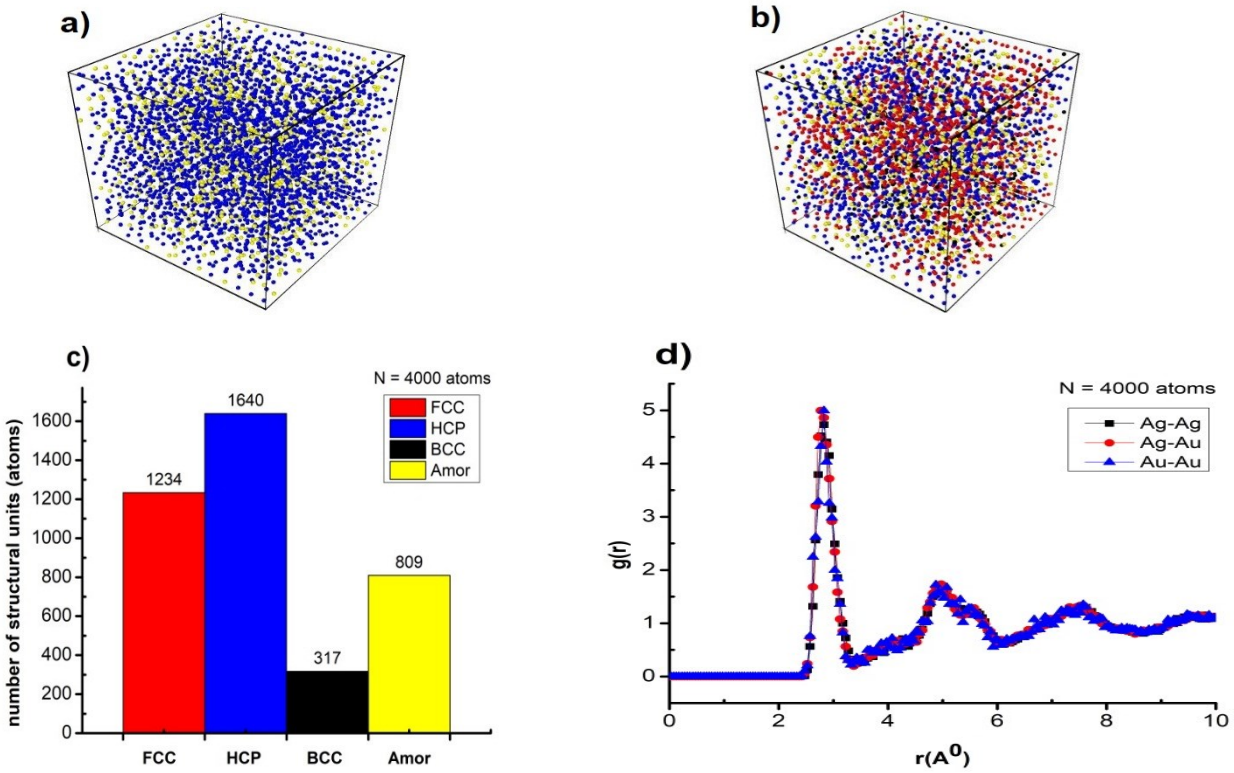

Figure 1. Alloy shape $Ag_{0.25}Au_{0.75}$ (a), structure shape (b), number of structural units (c), radial distribution function (d) of $Ag_{0.25}Au_{0.75}$ alloy at 300 K temperature

3.2. Effect of temperature

Observation in Figure 2 shows, the alloy $Ag_{0.25}Au_{0.75}$ at 300 K temperature has a structural shape (Figure 2a1) determined by the number of structural units 1234 FCC, 1640 HCP, 317 BCC, 809 Amor (Figure 2a2), the radial distribution function (RDF) has the lengths of the link Ag-Ag, Ag-Au, Au-Au respectively r = 2.83, 2.78, 2.83 Å with the height of the radial distribution function g(r) = 4.73, 5.00, 4.99 (Figure 2a3). When increasing the temperature from T = 300 K to T = 400, 500, 600, 700, 800, 900, 1000, 1100, 1200 K, the structure shape changes (Figure 2a1, 2b1, 2c1, .., 2k1), number of structural units FCC, HCP, Amor architecture changes. FCC decreased from 1234 FCC to 109 FCC, HCP decreased from 1640 HCP to 1211 HCP, BCC increased from 317 BCC to 767 BCC, Amor increased from 809 Amor to 2004 Amor (Figure 2a2, 2b2, 2c2, .., 2k2), and the radial distribution function changed as the Ag-bond lengths increased. Au has a constant value r = 2.78 Å, and the height of the radial distribution function from g(r) = 5.0 to g(r) = 3.1 (Figure 2a3, 2b3, 2c3,.., 2k3),. Through the obtained results, when the temperature is increased, the number of structural units FCC, HCP decreases, then BCC, Amor increases, which shows that when the alloy changes from solid state to a liquid state, the alloy $Ag_{0.25}Au_{0.75}$ tends to gradually shift to BCC structure, Amor is also the characteristic color of $Ag_{0.25}Au_{0.75}$ alloy at high temperature. In addition to the characteristics such as shape, structure shape and radial distribution function, there are other influencing factors that are the alloy size and the energy of the material changes, the results are shown in Table 2.

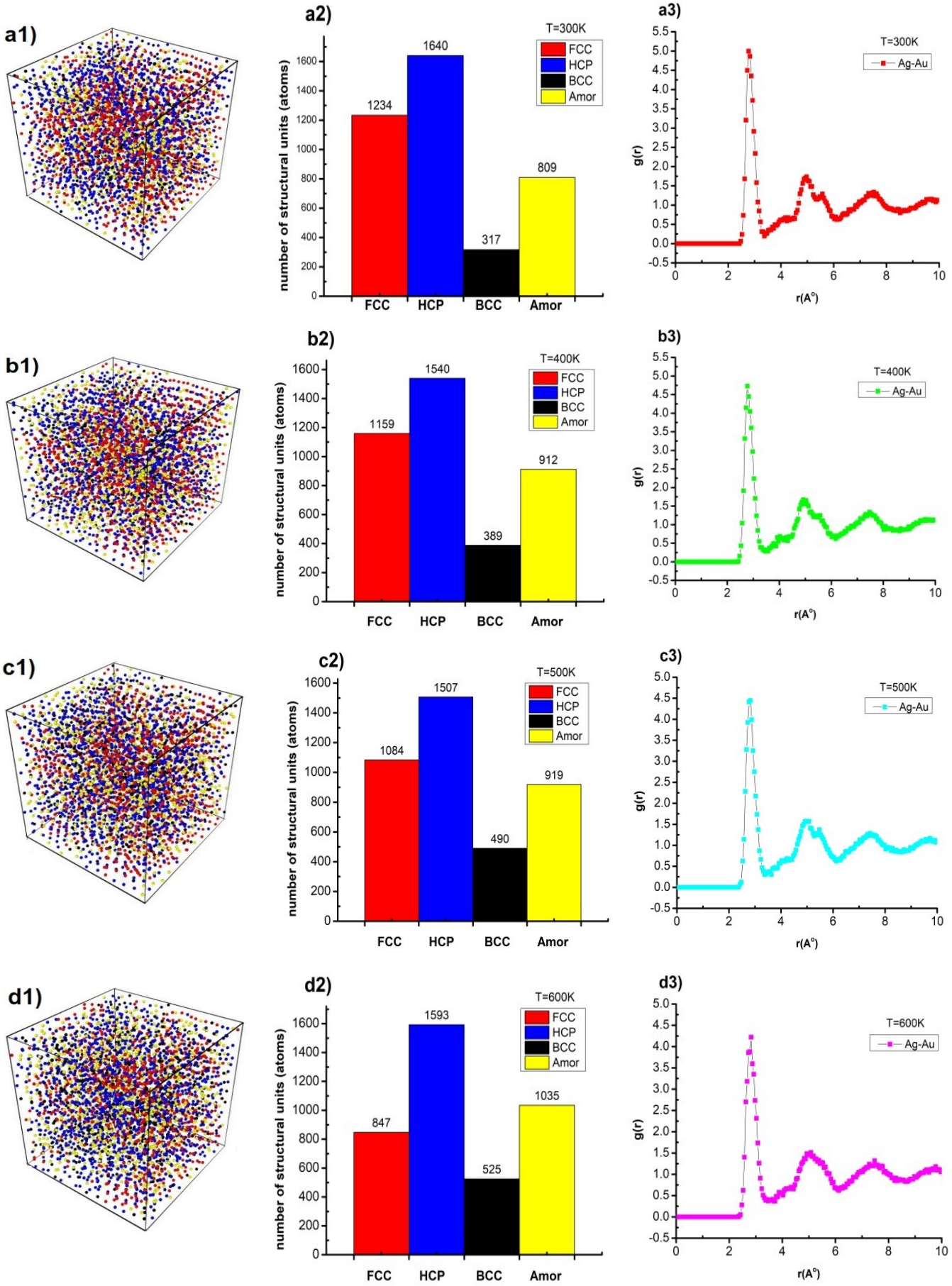
a1)
a2)
T=300K
FCC
HCP
BCC
Amor
1234
1640
317
809
number of structural units (atoms)
a3)
T=300K
Ag-Au
g(r)
r(A°)
b1)
b2)
T=400K
1159
1540
389
912
b3)
T=400K
c1)
c2)
T=500K
1084
1507
490
919
c3)
T=500K
d1)
d2)
T=600K
847
1593
525
1035
d3)
T=600K

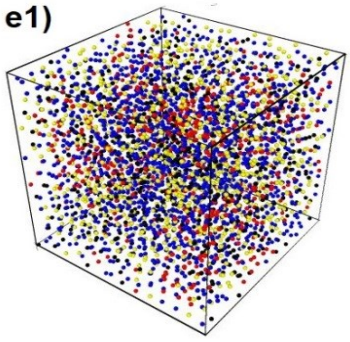
e1)

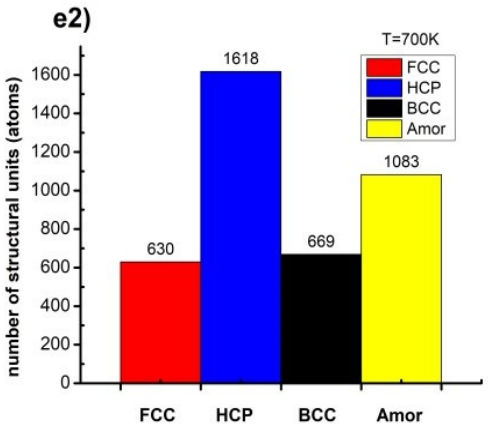
e2)
T=700K
FCC
HCP
BCC
Amor
1618
630
669
1083
number of structural units (atoms)
FCC
HCP
BCC
Amor

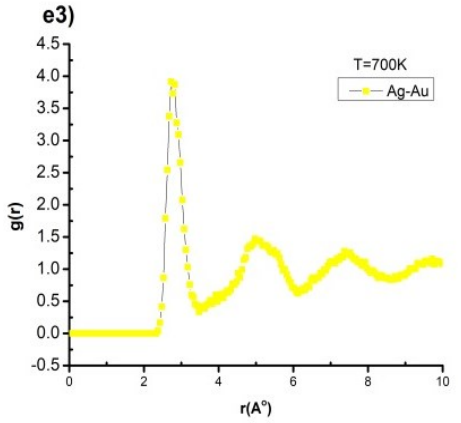
e3)
T=700K
Ag-Au
g(r)
r(A°)

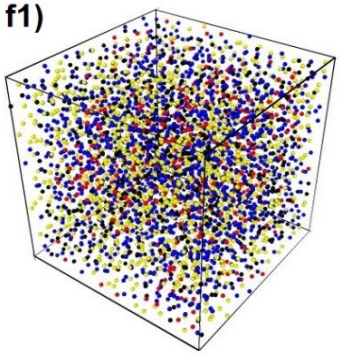
f1)

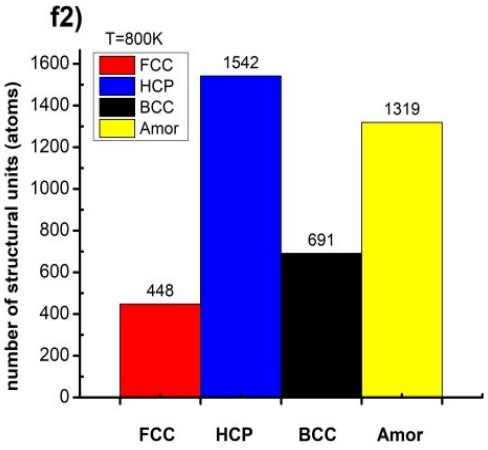
f2)
T=800K
FCC
HCP
BCC
Amor
1542
448
691
1319
number of structural units (atoms)
FCC
HCP
BCC
Amor

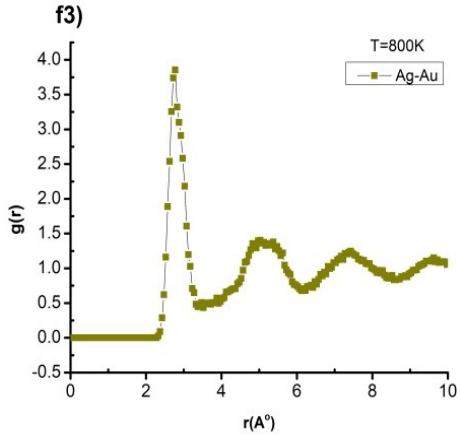
f3)
T=800K
Ag-Au
g(r)
r(A°)

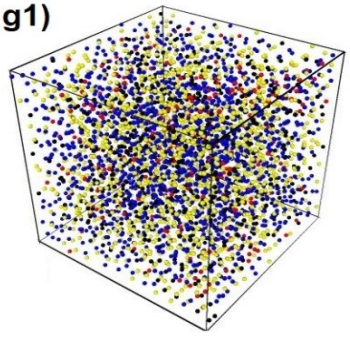
g1)

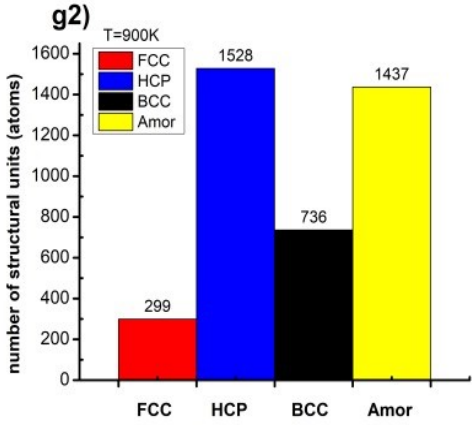
g2)
T=900K
FCC
HCP
BCC
Amor
1528
299
736
1437
number of structural units (atoms)
FCC
HCP
BCC
Amor

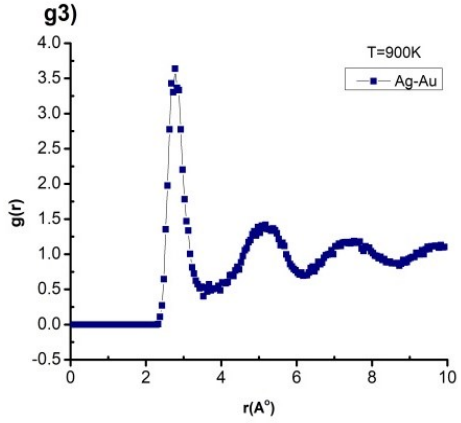
g3)
T=900K
Ag-Au
g(r)
r(A°)

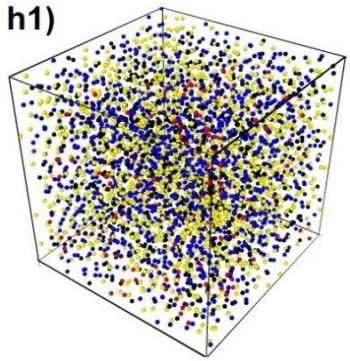
h1)

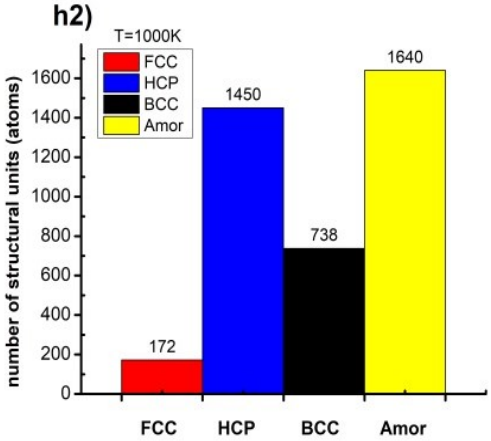
h2)
T=1000K
FCC
HCP
BCC
Amor
1450
172
738
1640
number of structural units (atoms)
FCC
HCP
BCC
Amor

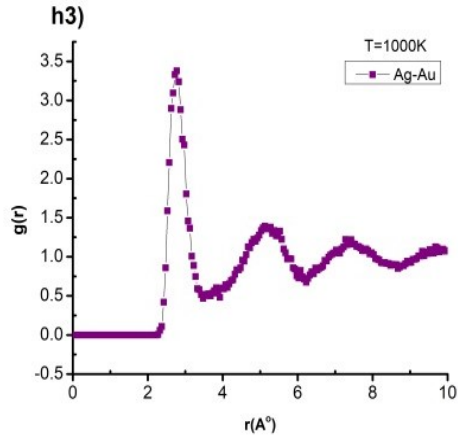
h3)
T=1000K
Ag-Au
g(r)
r(A°)

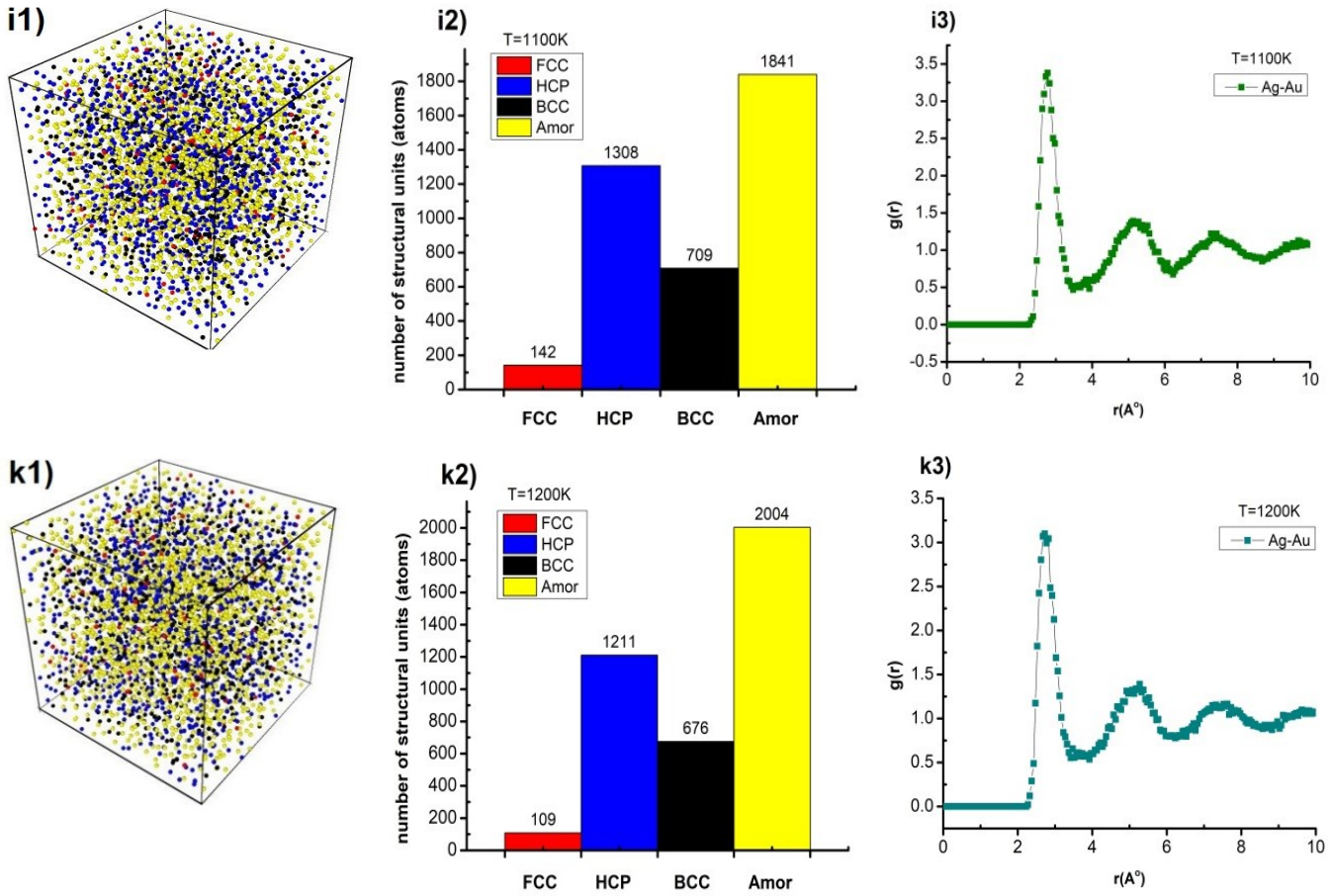

Figure 2. Structure shape (a1, b1, .., k1), number of structural units (a2, b2, .., k2), RDF radial distribution function (a3, b3, .., k3) of alloy $Ag_{0.25}Au_{0.75}$ at different temperatures

Table 2. Energy of system, size of alloy $Ag_{0.25}Au_{0.75}$ at different temperatures

T(K)	E_{tot} (eV)	l (nm)	T (K)	E_{tot} (eV)	l (nm)
300	-12073	40.85	**800**	-11732	40.855
400	-12003	40.851	**900**	-11654	40.856
500	-11932	40.852	**1000**	-11579	40.857
600	-11864	40.853	**1100**	-11485	40.858
700	-11798	40.854	**1200**	-11419	40.859

The results indicate that as the temperature increases, the size of the material undergoes minimal changes, remaining almost unchanged from l = 40.85 nm to l = 40.859 nm. In contrast, the total energy of the system increases rapidly from E_{tot} = -12073 eV to E_{tot} = -11419 eV (Table 2). These findings suggest that while the size of the alloy remains relatively stable with increasing temperature, the total energy of the system experiences significant growth. The number of FCC and HCP structural units also sharply decreases, while the number of BCC structural units decreases gradually. Additionally, the Amor fraction increases sharply, forming a mid-phase transition region from T = 800 K to T = 1000 K. This is because the number of units changes significantly within this range, leading to a marked change in the system's energy. These results can serve as a foundation for future experimental research on AgAu alloy materials, guiding their practical applications.

4. CONCLUSION

In this study, the temperature effect on the microstructural characteristics, phase transition by molecular dynamics method with Sutton-Chen and periodic boundary conditions on $Ag_{0.25}Au_{0.75}$ alloy. When increases the temperature, the number of structural units FCC, HCP, BCC, Amor all increase, which show that when the alloy has changed from solid state to liquid state. In addition, the Ag-Au bond length is almost constant, with r = 2.78 Å, the RDF height decreases. These obtained results can be aaplied for future application research and fabrication of $Ag_{0.25}Au_{0.75}$ alloy.

Author Contributions: Ştefan Ţălu: Writing-original draft & editing. Tran Quoc Tuan: Conceptualization, Methodology, Investigation, Validation, Writing-original draft-review & editing, Formal analysis. Ong Van Hoang, Vu Thi Ha, Tran Thi Duyen, Nguyen Thi Thu-Cuc: Writing-original draft, Formal analysis. All authors have read and agreed to the published version of the manuscript.

Funding: This research is funded by the University of Transport Technology (UTT), Hanoi, Viet Nam under grant number: ĐTTĐ2021-10.

Conflicts of Interest: The authors declare no conflict of interest.

ORCID:

Ştefan Ţălu, http://orcid.org/0000-0003-1311-7657.

Tuan Tran Quoc, https://orcid.org/0000-0002-3267-0696

Data Availability Statement: The data that supports the findings of this study are available within the article.

References

[1] L. Burr, I. Schubert, W. Sigle, C. Trautmann, M.E. Toimil-Molares. (2015). Surface Enrichment in Au-Ag Alloy Nanowires and Investigation of the Dealloying Process. *The Journal of Physical Chemistry C*, 119(36), 20949-20956.

[2] M. Zhou, J. Zhong, S. Wang, Q. Guo, M. Zhu, Y. Pei, A. Xia. (2015). Ultrafast Relaxation Dynamics of Luminescent Rod-Shaped, Silver Doped AgxAu25-x Clusters. *The Journal of Physical Chemistry C*, 119(32), 18790-18797.

[3] F. Munoz, A. Varas, J. Rogan, J.A. Valdivia, M. Kiwi. (2015). Au13-nAgn Clusters: A Remarkably Simple Trend. *Physical Chemistry Chemical Physics*, 17, 30492-30498.

[4] P. Wang, L. Lin, Z. Guo, J. Chen, H. Tian, X. Chen, H. Yang. (2016). Highly Fluorescent Gene Carrier Based on Ag-Au Alloy Nanoclusters. *Macromolecular Bioscience*, 16(1), 160-167.

[5] E. Seker, W.C. Shih, K.J. Stine. (2018). Nanoporous metals by alloy corrosion: Bioanalytical and biomedical applications. *MRS Bulletin*, 43, 49-56.

[6] Q. Chen, Y. Ding, M.W. Chen. (2018). Nanoporous metal by dealloying for electrochemical energy conversion and storage. *MRS Bulletin*, 43, 43-48.

[7] R.C. Newman, S.G. Corcoran, J. Erlebacher, M.J. Aziz, K. Sieradzki. (1999). Alloy corrosion. *MRS Bulletin*, 24, 24-28.

[8] J. Erlebacher. (2004). An atomistic description of dealloying porosity evolution, the critical potential, and rate-limiting behavior. *Journal of The Electrochemical Society*, 151(10), C614-C626.

[9] P. Liu, Q. Chen, Y. Ito, J. Han, S. Chu, X. Wang, K.M. Reddy, S. Song, A. Hirata, M. Chen. (2020). Dealloying Kinetics of AgAu Nanoparticles by In Situ Liquid-Cell Scanning Transmission Electron Microscopy. *Nano Letters*, 20(3), 1944-1951.

[10] P. Hu, Y. Song, L. Chen and S. Chen. (2015). Electrocatalytic activity of alkyne-functionalized AgAu alloy nanoparticles for oxygen reduction in alkaline media. *Nanoscale*, 7(21), 9627-9636.

[11] C.H. Cui and S.H. Yu. (2013). Accounts of Chemical Research, 46, 1427-1437.

[12] B. Lim, M.J. Jiang, P.H.C. Camargo, E.C. Cho, J. Tao, X.M. Lu, Y.M. Zhu and Y.N. Xia. (2009). Science, 324, 1302-1305.

[13] J.L. Zhang, M.B. Vukmirovic, K. Sasaki, A.U. Nilekar, M. Mavrikakis and R.R. Adzic, J. Am.

(2005). Chemical Society, 127, 12480-12481

[14] A. Satoh. (2011). Introduction to practice of Molecular Simulation. *Elsevier Inc.*

[15] J. Mostowski, M. Trippenbach and C.L. Van. (1987). Phase Space Approach to Two-electron Atom Ionisation. *Fourth International Conference on multiphoton processes, Boulder, Colorado*.

[16] M. Trippenbach, D. Thesis. (1987). Center of Theoretical Physics. *Polish Academy of Science*.

[17] C.L. Van, P. Goldstein. (2008). Concise Course in Nonlinear Partial Diferential Equations. *Zielona Góra*.

[18] N.T. Dung, N.C. Cuong, D.Q. Van, T.Q. Tuan. (2020). Study the effects of factors on the structure and phase transition of bulk Ag by molecular dynamics method. *International Journal of Computational Materials Science and Engineering*, 9(3), 2050016.

[19] N.T. Dung, C.L. Van, T. Ștefan. (2021). The Structure and Crystallizing Process of NiAu Alloy: A Molecular Dynamics Simulation Method. *Journal of Composites Science*, 5(1), 18.

[20] Z. Yanqiu, J. Shuyong. (2018). Atomistic mechanisms for temperature-induced crystallization of amorphous copper based on molecular dynamics simulation. *Computational Materials Science*, *151*, 25-33.

[21] D.E. Spearot, M.A. Tschopp, K.I. Jacob, D.L. McDowell. (2007). Tensile strength of < 1 0 0> and < 1 1 0> tilt bicrystal copper interfaces. *Acta Materialia*, *55*, 705-714.

[22] M.A. Tschopp, D.E. Spearot, D.L. McDowell. (2007). Atomistic simulations of homogeneous dislocation nucleation in single crystal copper. *Modelling and Simulation in Materials Science and Engineering*, *15*, 693-709.

[23] W.J. Murphy, A. Higginbotham, G. Kimminau, B. Barbrel, E.M. Bringa, J. Hawreliak, R. Kodama, M. Koenig, W. McBarron, M.A. Meyers, B. Nagler, N. Ozaki, N. Park, B. Remington, S. Rothman, S.M. Vinko, T. Whitcher, J.S. Wark. (2010). The strength of single crystal copper under uniaxial shock compression at 100 GPa. *Journal of Physíc: Condensed Matter*, *22(6)*, 065404.

[24] H. Rafii-Tabar, A.P. Sutton. (1991). Long-range Finnis-Sinclair potentials for f.c.c. metallic alloys. *Philosophical Magazine Letters*, 63, 217-224.

[25] Y. Kimura, Y. Qi, T. Cagın, Goddard III, W.A. (1998). The quantum Sutton-Chen many-body potential for properties of fcc metals. *Physical Review* – Citeseer.

[26] A.P. Sutton. (1990). Long-range finnis-sinclair potentials. *Philosophical Magazine Letters*, 61, 139-146.

[27] A. Januszko. (2015). Phonon spectra and temperature variation of bulk properties of Cu, Ag, Au and Pt using Sutton-Chen and modified Sutton-Chen potentials. *Journal of Physics and Chemistry of Solids*, 82, 67-75.

[28] L. Verlet. (1967). Computer "experiments" on classical fluids. I. Thermodynamical properties of Lennard-Jones molecules. *Physical Review B*, 159, 98-103.

[29] R. Ali, B. Kamran. (2017). Identification of crystal structures in atomistic simulation by predominant common neighborhood analysis, *Computational Materials Science*, 126, 182-190.

[30] S.A. Nose. (1984). Unified formulation of the constant temperature molecular dynamics methods. *The Journal of Chemical Physics*, 81(1), 511-519.

[31] W.G. Hoover. (1985). Canonical dynamics: equilibrium phase-space distributions. *Physical Review A,* 31(3), 1695-1697.